Vibrational and Electronic Spectroscopy of Electronically Excited Polychromophoric Ruthenium(II) Complexes

Carlo A. Bignozzi,*[1a] Roberto Argazzi,[1a] Claudio Chiorboli,[1a] Franco Scandola,[1a] R. Brian Dyer,[1b] Jon R. Schoonover,[1c] and Thomas J. Meyer*[1c]

Dipartimento di Chimica, Centro di Fotoreattività e Catalisi CNR, Università di Ferrara, 44100 Ferrara, Italy, Los Alamos National Laboratory, Los Alamos, New Mexico 87545, and Department of Chemistry, The University of North Carolina, Chapel Hill, North Carolina 27514

Received May 19, 1993[⊗]

The metal to ligand charge-transfer excited states of the polychromophoric complexes $[(NC)(bpy)_2Ru^{II}(CN)Ru^{II}(bpy)_2(CN)]^+$, $[(NC)(bpy)_2Ru^{II}(CN)Ru^{II}(phen)_2(CN)]^+$, $[(NC)(phen)_2Ru^{II}(CN)Ru^{II}(bpy)_2(CN)]^+$, $[(NC)(bpy)_2Ru^{II}(CN)Ru^{II}(bpy)_2(NC)Ru^{II}(bpy)_2(CN)]^{2+}$, and $[NC(bpy)_2Ru^{II}(CN)Ru^{II}(dcb)_2(NC)Ru(bpy)_2(CN)]^{2-}$ (bpy is 2,2′-bipyridine, phen is 1,10-phenanthroline, and dcb is 4,4′-dicarboxy-2,2′-bipyridine) and of model mononuclear complexes have been investigated in CH_3CN by time-resolved resonance Raman (TR^3) and transient UV/vis absorption spectroscopy. The observation in the TR^3 spectra of vibrations of a single type of reduced ligand and the cross check obtained by exchanging ligands around the metal centers provide unambiguous evidence for localization of the excited electron on the polypyridine ligand of the N-bonded (to bridging CN^-) chromophore. The presence of excited-state intervalence transfer bands has been inferred by the comparison of the transient absorbance spectra of the polynuclear complexes with the ground-state spectra of reduced and one-electron oxidized forms and with the spectra of the excited mononuclear complexes. These comparisons indicate the presence of distinct Ru(II) and Ru(III) centers in the excited states of the polynuclear complexes.

Introduction

In the past several years the synthesis and study of new polynuclear ruthenium polypyridine complexes has grown impressively, particularly in the light of the possibility of achieving photoinduced separation of redox equivalents or electronic energy transfer between components.[2-8] In the limit of a weak electronic interaction between the metal centers, appropriate variations of chromophoric[9-14] and nonchromophoric ligands[11,15-18] and metal oxidation states[19-22] allow the spectroscopic and photophysical properties of the component units to be modified. These transitions frequently determine the type of transfer process observed.[2]

Studies on polynuclear complexes based on cyano-bridged $Ru(bpy)_2^{2+}$ units (bpy is 2,2′-bipyridine) have indicated that, by synthetic control of the linkage, intramolecular energy transfer can be driven between metal-to-ligand charge transfer, MLCT, excited states localized on C- and N-bonded units.[20,22] This has led to the design of a molecular device for the visible sensitization of semiconductors[23,24] and to oligomers which are able to act as molecular conduits for long-range energy transfer.[25] In the latter case the processes that occur following electronic excitation are

⊗ Abstract published in *Advance ACS Abstracts,* March 1, 1994.

(1) (a) Università di Ferrara. (b) Los Alamos National Laboratory. (c) The University of North Carolina.

(2) For recent reviews and articles of general interest see refs 2–8 (a) Meyer, T. J. *Acc. Chem. Res.* **1989**, *22*, 163. (b) Scandola, F.; Indelli, M. T.; Chiorboli, C.; Bignozzi, C. A. *Top. Curr. Chem.* **1990**, *158*, 73. (c) Balzani, V.; Scandola, F. *Supramolecular Photochemistry*; Horwood: Chichester, U.K., 1991; Chapters 5 and 6. (d) Kalyanasundaram, K. *Photochemistry of Polypyridine and Porphyrin Complexes*; Academic Press: London, 1992; Chapters 5 and 6.

(3) (a) Lei, Y.; Buranda, T.; Endicott, J. F. *J. Am. Chem. Soc.* **1990**, *112*, 8820. (b) Buranda, T.; Ley, Y.; Endicott, J. F. *J. Am. Chem. Soc.* **1992**, *114*, 6916. (c) Song, X.; Ley, Y.; Van Wallendal, S.; Perkovic, M. W.; Jackman, D. C.; Endicott, J. F.; Rillema, D. P. *J. Phys. Chem.* **1993**, *97*, 3225.

(4) (a) Rillema, D. P.; Sahai, R.; Matthews, P.; Edwards, A. K.; Shaver, R. L.; Morgan, L. *Inorg. Chem.* **1990**, *29*, 167. (b) Wallendael, S. V.; Rillema, D. P. *Coord. Chem. Rev.* **1991**, *111*, 297. (c) Kalyanasundaram, K.; Gratzel, M.; Nazeeruddin, Md. K. *Inorg. Chem.* **1992**, *31*, 5243.

(5) Petersen, J. D.; Morgan, L. W.; Hsu, I.; Billadeau, M. A.; Ronco, S. E. *Coord. Chem. Rev.* **1991**, *111*, 319.

(6) (a) Schmehl, R. H.; Auerbach, R. A.; Wacholtz, W. F. *J. Phys. Chem.* **1988**, *92*, 6202. (b) Shaw, J. R.; Webb, R. T.; Schmehl, R. H. *J. Am. Chem. Soc.* **1990**, *112*, 1117.

(7) (a) Denti, G.; Serroni, S.; Campagna, S.; Juris, A.; Ciano, M.; Balzani, V. In *Perspectives in Coordination Chemistry*; Williams, A. F., Floriani, C., Maerbach, A. E., Eds., Verlag: Basel, 1992; p 153. (b) Denti, G.; Campagna, S.; Serroni, S.; Ciano, M.; Balzani, V. *J. Am. Chem. Soc.* **1992**, *114*, 2944. (c) De Cola, L.; Barigelletti, F.; Balzani, V.; Belser, P.; von Zelewsky, A.; Seel, C.; Frank, M.; Voegtle, F. In *Supramolecular Chemistry*; Balzani, V., De Cola, L., Eds.; Kluwer: Dordrecht, The Netherlands, 1992, p 157. (d) Serroni, S.; Denti, G.; Campagna, S.; Juris, A.; Ciano, M.; Balzani, V. *Angew. Chem., Int. Edit. Engl.* **1992**, *31*, 1493.

(8) (a) Worl, L. A.; Strauss, G. F.; Younathan, J. N.; Baxter, S. M.; Meyer, T. J. *J. Am. Chem. Soc.* **1990**, *112*, 7571. (b) Baxter, S. M.; Jones, W. E., Jr.; Danieldson, E.; Worl, L.; Strouse, J.; Younathan, J.; Meyer, T. J. *Coord. Chem. Rev.* **1991**, *111*, 47.

(9) Meyer, T. J. *Pure Appl. Chem.* **1986**, *58*, 1193.

(10) Krausz, E.; Ferguson, J. *Prog. Inorg. Chem.* **1989**, *37*, 293.

(11) Juris, A.; Barigelletti, F.; Balzani, V.; Campagna, S.; Belser, P.; von Zelewsky, A. *Coord. Chem. Rev.* **1988**, *84*, 85.

(12) Johnson, J. R.; Westmoreland, T. D.; Caspar, J. V.; Barqawi, K. R.; Meyer, T. J. *Inorg. Chem.* **1988**, *27*, 3195.

(13) Barqawi, K. R.; Llobet, A.; Meyer, T. J. *J. Am. Chem. Soc.* **1988**, *110*, 7751.

(14) Masui, H.; Lever, A. B. P.; Dodsworth, E. S. *Inorg. Chem.* **1993**, *32*, 258.

(15) Caspar, J. V.; Meyer, T. J. *Inorg. Chem.* **1983**, *22*, 2444.

(16) (a) Indelli, M. T.; Bignozzi, C. A.; Marconi, A.; Scandola, F. *J. Am. Chem. Soc.* **1988**, *110*, 7381. (b) Scandola, F.; Indelli, M. T. *Pure Appl. Chem.* **1988**, *60*, 973.

(17) Bignozzi, C. A.; Chiorboli, C.; Murtaza, Z.; Jones, W. E.; Meyer, T. J. *Inorg. Chem.* **1993**, *32*, 1036.

(18) Kalyanasundaram, K.; Nazeeruddin, Md. K. *Chem. Phys. Lett.* **1992**, *193*, 292.

(19) Curtis, J. C.; Bernstein, J. S.; Meyer, T. J. *Inorg. Chem.* **1985**, *24*, 385.

(20) Bignozzi, C. A.; Roffia, S.; Chiorboli, C.; Davila, S.; Indelli, M. T.; Scandola, F. *Inorg. Chem.* **1989**, *28*, 4350.

(21) Belser, P.; Von Zelewski, A.; Frank, M.; Steel, C.; Vogtle, F.; De Cola, L.; Barigelletti, F.; Balzani, V. *J. Am. Chem. Soc.* **1993**, *115*, 4076.

(22) Bignozzi, C. A.; Argazzi, R.; Schoonover, J. R.; Gordon, K. C.; Dyer, R. B.; Scandola, F. *Inorg. Chem.* **1992**, *31*, 5260.

(23) Amadelli, R.; Argazzi, R.; Bignozzi, C. A.; Scandola, F. *J. Am. Chem. Soc.* **1990**, *112*, 7099.

(24) Nazeeruddin, Md. K.; Liska, P.; Moser, J.; Vlachopoulos, N.; Gratzel, M. *Helv. Chim. Acta* **1990**, *73*, 1788.

(25) Bignozzi, C. A.; Argazzi, R.; Garcia, G. C.; Scandola, F.; Schoonover, J. R.; Meyer, T. J. *J. Am. Chem. Soc.* **1992**, *114*, 8727.

0020-1669/94/1333-1652$04.50/0

Scheme 1

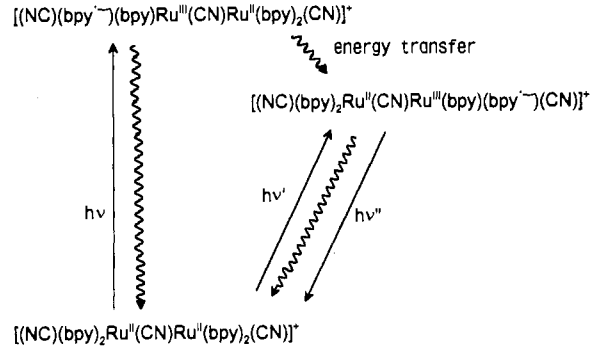

analyzed in Scheme 1 for the simplest member of this class, $[(NC)(bpy)_2Ru^{II}(CN)Ru^{II}(bpy)_2(CN)]^+$.

Cyanide as a bridging ligand is capable of supporting strong electronic coupling, but excited-state localization has been suggested for this complex by the similarity between the excited-state infrared spectrum of $[(NC)Ru^{II}(bpy)_2(CN)Ru^{II}(bpy)_2(CN)]^{+*}$ in the cyanide stretching region with the spectrum of the chemically prepared mixed-valence complex $[(NC)Ru^{II}(bpy)_2(CN)Ru^{III}(bpy)_2(CN)]^{2+}$.[22]

We report here excited-state Raman spectra of the complexes $[(NC)(phen)_2Ru^{II}(CN)Ru^{II}(bpy)_2(CN)]^+$, $[(NC)(bpy)_2Ru^{II}(CN)Ru^{II}(phen)_2(CN)]^+$, and $[(NC)(bpy)_2Ru^{II}(CN)Ru^{II}(dcb)_2(NC)Ru^{II}(bpy)_2(CN)]^{2-}$ (phen is 1,10-phenanthroline, dcb is 4,4'-dicarboxy-2,2'-bipyridine) which provide conclusive evidence for localization of the excitation energy on the unit that is N-bonded to the bridging cyano groups. We also note that the absorption features observed in the excited states of these complexes, and of a series of related polynuclear complexes, can be explained on the basis of a localized excitation model. A partial preliminary account of these results has been previously given.[26]

Experimental Section

Materials. Acetonitrile (Aldrich, gold label) and D_2O (Fluka) were used for spectroscopic measurements.

Complexes. The compounds and salts $Ru(bpy)_2(CN)_2$,[27] $[N(n\text{-}C_4H_9)_4]_4[Ru(dcb)_2(CN)_2]$,[22] $[(NC)(bpy)_2Ru(CN)Ru(bpy)_2(CN)](PF_6)$,[20] $[(NC)(bpy)_2Ru(CN)Ru(bpy)_2(NC)Ru(bpy)_2(CN)](PF_6)_2$,[20] $[(NC)(bpy)_2Ru(CN)Ru(phen)_2(CN)](PF_6)$,[20] $[N(n\text{-}C_4H_9)_4]_2[NC(bpy)_2Ru(CN)Ru(dcb)_2(NC)Ru(bpy)_2(CN)]$,[23] and $Na_2[(NC)(bpy)_2Ru(CN)Ru(dcb)_2(NC)Ru(bpy)_2(CN)]$[23] were available from previous studies. The complex $[(NC)(phen)_2Ru(CN)Ru(bpy)_2(CN)](PF_6)$ was prepared by the reaction between $Ru(phen)_2(CN)_2$[20] and $[Ru(bpy)_2(CN)(CH_3OH)]^+$ by following the procedures previously reported for $[(NC)(bpy)_2Ru(CN)Ru(bpy)_2(CN)](PF_6)$.[20]

Acetonitrile solutions of the mixed-valence complexes $[(NC)(bpy)_2Ru^{II}(CN)Ru^{III}(bpy)_2(CN)]^{2+}$, $[(NC)(bpy)_2Ru^{II}(CN)Ru^{III}(phen)_2(CN)]^{2+}$, $[(NC)(phen)_2Ru^{II}(CN)Ru^{III}(bpy)_2(CN)]^{2+}$, and $[(NC)(bpy)_2Ru^{II}(CN)Ru^{III}(bpy)_2(NC)Ru^{II}(bpy)_2(CN)]^{3+}$ were prepared by chemical oxidation of the reduced forms with a slight excess of bromine in acetonitrile.[22] For solubility reasons, the mixed-valence complex $[(NC)(bpy)_2Ru^{II}(CN)Ru^{III}(dcb)_2(NC)Ru^{II}(bpy)_2(CN)]^-$ was generated by addition of Br_2, from a standardized solution of Br_2 in acetonitrile,[28] to D_2O solutions of the reduced form of the complex.

Apparatus and Procedures. Cyclic voltammetric measurements were performed in acetonitrile solutions in the presence of 0.1 M tetraethylammonium tetrafluoroborate, $(NEt_4)BF_4$, a Pt working electrode, and an SCE reference electrode. Electrochemical, absorption, emission, and lifetime measurements were carried out as described previously.[20,22]

Transient absorbance difference spectra were measured by using an Applied Photophysics detection system with a J&K System 2000 frequency-doubled ruby laser, delivering 25-ns (half-width) pulses of 347-nm radiation. The maximum absorbance changes observed following the laser pulse were recorded as a function of wavelength at 10-nm intervals between 360 and 860 nm. The transient signals were corrected for variations in the laser pulse intenstiy by deflecting a small fraction of the laser beam to a photodiode whose output was calibrated against the benzophenone triplet absorption. Corrections of the intensities of these signals were also made for finite laser pulse duration by comparison with a calibration curve of intensity *vs* lifetime, obtained by quenching the triplet of benzophenone with oxygen in benzene solutions.

The difference spectra were converted into molar absorptivity changes, to give the absorption of the excited state (ESA), by standardization against absorbance-matched solutions of benzophenone in benzene (molar absorptivity of benzophenone triplet at 532 nm, 7630 M^{-1} cm^{-1}). In these experiments the concentration of the complexes ((1–2) × 10^{-4} M) was always higher than the concentration of adsorbed photons in the reaction cell ((3–7)) × 10^{-5} M).

Solutions of $Zn(ClO_4)_2$ in acetonitrile were standardized by atomic absorption spectroscopy by using a Perkin-Elmer Model 608 atomic absorption spectrophotometer.

Near-UV resonance Raman spectra were measured at CLS-4 (Los Alamos National Laboratory) using a Spectra-Physics Model 2045 Ar^+ laser with a SPEX 1877 triple spectrometer equipped with liquid-nitrogen-cooled Photometrics CCD.

Transient Raman spectra were measured at the UNC laser facility using the third harmonic (354.7 nm) of a Quanta-Ray DCR-2A pulsed Nd:YAG laser to both create the excited state and use as a source for the Raman scattering. The samples were degassed by several cycles of freeze–pump–thawing and sealed in an NMR tube. The scattered radiation was collected in a 135° backscattering geometry into a SPEX 1877 triple spectrometer equipped with an 1800 grooves/mm grating. The sigal was examined by a Princeton Instruments IRY-700G optical multichannel analyzer operating in the gated mode with a ST-110 OSMA detector controller. Timing was controlled by a Princeton Instruments FG-100 pulse generator. The final spectra were the result of 16 min of total integration time. Laser power was between 3 and 5 mJ per pulse. Data collection and storage were controlled by an IBM AT using a Princeton Instruments SMA software package.

Emission spectral fitting data were obtained by following an established protocol,[29] with a least-squares program based on a Simplex algorithm written by J. P. Claude.[30]

Results

Spectroscopic, Photophysical, and Redox Properties. Spectroscopic, photophysical, and redox properties for the complexes $Ru(bpy)_2(CN)_2$, $[(NC)(bpy)_2Ru^{II}(CN)Ru^{II}(bpy)_2(CN)]^+$, $[(NC)(bpy)_2Ru^{II}(CN)Ru^{II}(phen)_2(CN)]^+$, $[(NC)(bpy)_2Ru^{II}(CN)Ru^{II}(bpy)_2(CN)]^+$, and $[(NC)(bpy)_2Ru^{II}(CN)Ru^{II}(dcb)_2(NC)Ru^{II}(bpy)_2(CN)]^{2-}$ have been reported previously.[20,22,23] The assignments of oxidation states at the metal in these complexes are based on previously reported spectroscopic and electrochemical results.[20,22,23,31,32] Except for very small shifts in band maxima and intensity, the spectral featurs observed for $[(NC)(phen)_2Ru^{II}(CN)Ru^{II}(bpy)_2(CN)]^+$ in acetonitrile are the same as those for $[(NC)(bpy)_2Ru^{II}(CN)Ru^{II}(phen)_2(CN)]^+$. This comparison allows for the assignment of bands for $[(NC)(phen)_2Ru^{II}(CN)Ru^{II}(bpy)_2(CN)]^+$ at 263 (ϵ = 73 900) and 288 nm (ϵ = 50 000) to π–π^*(phen) and π–π^*(bpy) transitions, respectively. The visible absorption bands (λ_{max} = 480 nm, ϵ = 16 600) are convolutions of MLCT dπ–π^*(bpy) and dπ–π^*(phen) bands. In cyclic voltammograms of $[(NC)(phen)_2Ru^{II}(CN)Ru^{II}(bpy)_2(CN)]^+$, two one-electron reversible waves appear at 0.72 and 1.35 V *vs* SCE for the two $Ru^{III/II}$ couples, as well a series of π^*(bpy)- and π^*(phen)-based reductions. As for the analogous oligomers, the first oxidative process can be confidently assigned to oxidation of the N-bonded

(26) Bignozzi, C. A.; Argazzi, R.; Chiorboli, C.; Roffia, S.; Scandola, F. *Coord. Chem. Rev.* **1991**, *111*, 261.
(27) Demas, J. N.; Turner, T. F.; Crosby, G. A. *Inorg. Chem.* **1969**, *8*, 674.
(28) Powers, M. J.; Callahan, R. W.; Salmon, D. J.; Meyer, T. J. *Inorg. Chem.* **1976**, *15*, 894.
(29) (a) Caspar, J. V.; Meyer, T. J. *J. Am. Chem. Soc.* **1983**, *105*, 5583. (b) Kober, E. M.; Caspar, J. V.; Lumpkin, R. S.; Meyer, T. J. *J. Phys. Chem.* **1986**, *90*, 3722. (c) Worl, L. A.; Duessing, R.; Chen, P.; Della Ciana, L.; Meyer, T. J. *J. Chem. Soc., Dalton Trans.* **1991**, 849.
(30) Claude, J. P. Manuscript in preparation.
(31) Roffia, S.; Casadei, R.; Paolucci, F.; Paradisi, C.; Bignozzi, C. A.; Scandola, F. *J. Electroanal. Chem.* **1991**, *302*, 157.
(32) Teixeira, M. G.; Roffia, S.; Bignozzi, C. A.; Paradisi, C.; Paolucci, F. *J. Electroanal. Chem.* **1993**, *345*, 243.

Table 1. Electrochemical and Photophysical Properties in CH_3CN at 298 K

complex	$E^{ox}_{1/2}$,[a] V	$E^{red}_{1/2}$,[a] V	E_{em}, 10^{-3} cm^{-1}	ΔG^0_{ES},[b] V	$^*E^{red}$,[c] V	τ,[d] ns	E_0,[e] 10^{-3} cm^{-1}	S_M[e]	$\Delta\bar{\nu}_{0,1/2}$,[e] 10^{-3} cm^{-1}
$Ru(bpy)_2(CN)_2$	0.86[f]	−1.62	14.5[f]	2.01	0.39	240[f]	14.7	0.49	1.84
$Ru(phen)_2(CN)_2$	0.88[f]	−1.62	14.9[f]	2.05	0.43	1200[f]	15.0	0.44	1.87
$[(NC)Ru(bpy)_2(CN)Ru(bpy)_2(CN)]^+$	0.74[f] 1.35	−1.54	14.0[f]	2.01	0.47	120[f]	14.1	0.34	2.14
$[(NC)Ru(phen)_2(CN)Ru(bpy)_2(CN)]^+$	0.72 1.35	−1.56	14.0	1.97	0.41	95	14.1	0.3	2.01
$[(NC)Ru(bpy)_2(CN)Ru(phen)_2(CN)]^+$	0.75[f] 1.35	−1.54	14.3[f]	1.99	0.45	400[f]	14.4	0.31	1.95
$[(NC)Ru(bpy)_2(CN)Ru(bpy)_2(NC)Ru(bpy)_2(CN)]^{2+}$	0.66[f] 1.19 1.46	−1.53	13.6[f]	1.97	0.44	90[f]	13.7	0.24	2.23
$[Zn(NC)Ru(bpy)_2(CN)Ru(bpy)_2(NC)Ru(bpy)_2(CN)Zn]^{6+}$	0.75 1.47 1.64		14.5	1.97		160	14.3	0.41	1.95
$[(NC)Ru(bpy)_2(CN)Ru(dcb)_2(NC)Ru(bpy)_2(CN)]^{2-}$	0.54[f] 1.24 1.58	−1.61	13.9[f]	1.92	0.31	140[f]	14.0	0.55	1.84

[a] Half-wave potentials vs SCE in 0.1M $[NEt_4](BF_4)$; consecutive oxidation potentials for the polynuclear complexes are in the format $E^{ox}_{1/2}(1)$, $E^{ox}_{1/2}(2)$, $E^{ox}_{1/2}(3)$, from the top to the bottom; $E^{red}_{1/2}$ is the potential of the first ligand-base reduction. [b] Calculated from emission spectral fitting parameters (see text). [c] Calculated from eq 2 (see text). [d] ±5%. [e] Obtained from the spectral fitting of the emission spectra (see text). [f] From ref 22.

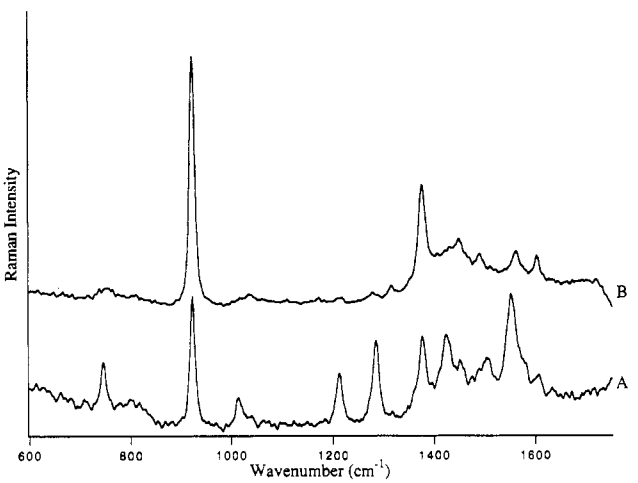

Figure 1. Time-resolved resonance Raman spectra of (A) $[(NC)(phen)_2Ru^{II}(CN)Ru^{II}(bpy)_2(CN)]^+$ and (B) $[(NC)(bpy)_2Ru^{II}(CN)Ru^{II}(phen)_2(CN)]^+$ in acetonitrile at room temperature. The frequencies of the Raman bands are compared in Table 2 to data for $[Ru(bpy)_3]^{2+}$ and $[Ru(phen)_3]^{2+}$. The spectra were measured by using the laser output at 354.7 nm both to excite the sample and to use as a source for Raman scattering. The spectra were the result of 16 min of total integration time.

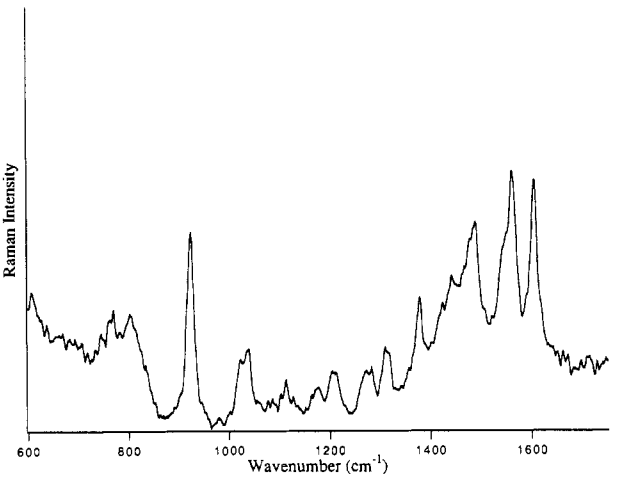

Figure 2. Transient resonance Raman spectrum of $[(NC)(bpy)_2Ru^{II}(CN)Ru^{II}(dcb)_2(NC)Ru^{II}(bpy)_2(CN)]^{2-}$ in acetonitrile. Conditions are as in Figure 1 and the Experimental Section.

Ru^{II} center.[20,22,31] Emission from $[(NC)(phen)_2Ru^{II}(CN)Ru^{II}(bpy)_2(CN)]^+$ and the other polynuclear complexes[20,22,23] was red-shifted with respect to those of the monomers. Excitation spectra matched the absorption spectra in all cases. Emission decay from $[(NC)(phen)_2Ru^{II}(CN)Ru^{II}(bpy)_2(CN)]^+$ was exponential with $\tau = 95$ ns. Photophysical and redox properties for the series are reported in Table 1.

Time-Resolved Resonance Raman. The transient Raman spectra of $[(NC)(phen)_2Ru^{II}(CN)Ru^{II}(bpy)_2(CN)]^+$ and $[(NC)(bpy)_2Ru^{II}(CN)Ru^{II}(phen)_2(CN)]^+$ measured at room temperature in acetonitrile are shown in Figure 1 with $[(NC)(bpy)_2Ru^{II}(CN)Ru^{II}(dcb)_2(NC)Ru^{II}(bpy)_2(CN)]^{2-}$ in Figure 2. These spectra were obtained under identical conditions by utilizing 354.7-nm laser pulses to both excite the sample and interrogate the excited state. The frequencies of the Raman bands in Figure 1 are listed in Table 2 and compared with data for $[Ru(bpy)_3]^{2+}$ and $[Ru(phen)_3]^{2+}$.[33-37] The ground- and excited-state data for $[Ru(dcb)_2(CN)_2]^{4-}$ and the trimer are compared in Table 3.

Excited-State Redox Potentials. Excited-state redox potentials were estimated from ground-state potentials measured by cyclic voltammetry and the emission spectral fitting parameters from eqs 1 and 2. In these equations the quantity $[E_0 + (\Delta\bar{\nu}_{0,1/2})^2/16k_bT\ln 2]$ is the free energy of the excited state above the ground state, ΔG^0_{ES},[29c] and $E^{ox}_{1/2}$ and $E^{red}_{1/2}$ are the ground-state potentials for the $Ru^{III/II}$ couple and the first ligand-based reduction. For the polynuclear complexes the first reduction is a multielectron process as shown by the higher peak current with respect to one-electron oxidation wave and the difference between

$$^*E^{ox} = E^{ox}_{1/2} - [E_0 + (\Delta\bar{\nu}_{0,1/2})^2/16k_bT\ln 2] \quad (1)$$

$$^*E^{red} = E^{red}_{1/2} + [E_0 + (\Delta\bar{\nu}_{0,1/2})^2/16k_bT\ln 2] \quad (2)$$

(33) (a) Bradley, P. G.; Kress, N.; Hornberger, B. A.; Dallinger, R. F.; Woodruff, W. H. *J. Am. Chem. Soc.* **1981**, *103*, 7441. (b) Dallinger, R. F.; Woodruff, W. H. *J. Am. Chem. Soc.* **1979**, *101*, 4391.

(34) (a) Strommen, D. P.; Mallick, P. K.; Danzer, G. D.; Lumpkin, R. S.; Kincaid, J. R. *J. Phys. Chem.* **1990**, *94*, 1357. (b) Mallick, P. K.; Strommen, D. P.; Kincaid, J. R. *J. Am. Chem. Soc.* **1990**, *112*, 1686.

(35) (a) Mabrouk, P. A.; Wrighton, M. S. *Inorg. Chem.* **1986**, *25*, 526. (b) Smothers, W. K.; Wrighton, M. S. *J. Am. Chem. Soc.* **1983**, *105*, 1067.

(36) Chang, X. J.; Xu, X.; Yabe, T.; Yu, S.-C.; Anderson, D. R.; Orman, L. K.; Hopkins, J. B. *J. Phys. Chem.* **1990**, *94*, 729.

(37) Kumar, C. V.; Barton, J. K.; Turro, N. J.; Gould, I. R. *Inorg. Chem.* **1987**, *26*, 1455.

Table 2. Raman Energies in cm^{-1} from Transient Spectra of $[(NC)(phen)_2Ru^{II}(CN)Ru^{II}(bpy)_2(CN)]^+$ and $[(NC)(bpy)_2Ru^{II}(CN)Ru^{II}(phen)_2(CN)]^+$ Compared to Data from Spectra of $[Ru^{II}(bpy)_3]^{2+}$ and $[Ru^{II}(phen)_3]^{2+}$ in CH_3CN at 298 K[a]

$[(NC)(phen)_2Ru^{II}(CN)Ru^{II}(bpy)_2(CN)]^+$	$[(NC)(bpy)_2Ru^{II}(CN)Ru^{II}(phen)_2(CN)]^+$	$[Ru^{II}(bpy)_3]^{2+}$	$[Ru^{II}(phen)_3]^{2+}$	origin
745 s	748 m	745 s	745 m	b*,p*
1014 m		1012 m		b*
	1033 w			b
	1107 w			b
			1150 m	p
	1172 w			b
1212 s		1212 s		b*
	1210 w		1209 w	p*
	1278 w			b
1285 s		1283 s		b*
	1315 m		1312 m	p*
	1320 m	1320 m		b
1365 w		1364 w		b*
1424 s		1424 s		b*
	1432 m		1434 s	p*
1450 m	1450 s	1450 w		b,p
	1455 sh		1455 s	p*
	1490 s	1488 w		b
1495 m		1495 m		b*
1506 m		1506 m		b*
	1515 w		1520 m	p*
1549 s		1549 s		b*
	1562 m			p
	1583 m		1584 s	p*
1606 w	1604 m	1606 m	1606 sh	b,p
1632 w			1632 m	p

[a] 354.7-nm laser pulses were used for excitation and as a source for the Raman scattering. s, m, and w denote the relative intensities of the Raman bands as strong, medium, or weak. b and p label the origin of ground-state bands from bpy and phen, respectively, while an asterisk labels an excited-state band and sh a band as a shoulder on another band.

Table 3. Raman Bands in cm^{-1} from Transient Spectra of $[(NC)(bpy)_2Ru^{II}(CN)Ru^{II}(dcb)_2(NC)Ru^{II}(bpy)_2(CN)]^{2-}$ Compared to Ground- and Excited-State Data for $[Ru^{II}(dcb)_2(CN)_2]^{4-}$ in CH_3CN or H_2O at 298 K[a]

$[(NC)(bpy)_2Ru^{II}(CN)Ru^{II}(dcb)_2(NC)Ru^{II}(bpy)_2(CN)]^{2-}$		$[Ru^{II}(dcb)_2(CN)_2]^{4-}$		
pulsed 354.7 nm	cw 363.8 nm	pulsed 354.7 nm	cm 363.8 nm	origin
1024	1024	1020		dcb,dcb*
	1030		1029	dcb
1039		1042		b,dcb*
1113	1112			dcb*
1177	1174			b
1211		1214		dcb*
			1255	dcb
	1263			b
1272	1276			b
1289		1290		dcb*
			1295	dcb
1315	1313	1315		dcb*,b
	1373		1373	dcb
	1430		1430	dcb
1446		1444		dcb*
			1478	dcb
1488	1488	1489		dcb*,b
1548	1542	1552	1545	dcb,dcb*
1561	1560			b
1605	1606			b
		1618	1618	dcb

[a] For the transient spectra, 354.7-nm laser pulses were used both for excitation and as a source for Raman scattering. The ground-state spectra were measured with 363.8-nm laser light. The labels b and dcb signify the origin of ground-state peaks as bpy or dcb, respectively; an asterisk signifies an excited-state peak.

the cathodic and anodic peak potentials of 100–130 mV. The multielectron charcter is due to the reduction of polypyridine ligands on different metals at overlapping potentials.[31,32] For $[(NC)(bpy)_2Ru^{II}(CN)Ru^{II}(bpy)_2(CN)]^+$ and $[(NC)(bpy)_2Ru^{II}(CN)Ru^{II}(bpy)_2(NC)Ru^{II}(bpy)_2(CN)]^{2+}$,[31] deconvolution of the first reduction wave in DMF at −54 °C indicated that the two-electron process observed for $[(NC)(bpy)_2Ru^{II}(CN)Ru^{II}(bpy)_2(CN)]^+$ and the three-electron process for $[(NC)(bpy)_2Ru^{II}(CN)Ru^{II}(bpy)_2(NC)Ru^{II}(bpy)_2(CN)]^{2+}$ consist of one-electron waves separated by about 50 mV. This difference can be attributed to differences in the π^*-accepting bpy orbitals since electronic interactions between ligands at different metals is expected to be negligible. The first reduction is expected to occur at a bpy ligand bound to a Ru C-bonded to the bridging cyanide since C-bonding stabilizes π^*(bpy) by greater $d\pi$–π^* mixing. Since the lowest ^{3}MLCT excited state is at the N-bonded units[20,22,31] (see Discussion), the use of eq 2 requires a small correction. In the calculations of excited-state redox potentials, $E_{1/2}^{red}$ values have been taken at the midpoint between peak potentials for the reductive and oxidative waves.

Emission spectra at room temperature in CH_3CN were subjected to a Frank–Condon analysis based on a single mode approximation (eq 3).[29]

$$I(\bar{\nu}) = \sum_{\upsilon_M=0}^{5}\left[\left(\frac{E_0 - \upsilon_M\hbar\omega_M}{E_0}\right)^3 \frac{S_M^{\upsilon_M}}{\upsilon_M!} \times \exp\left\{-4\ln 2\left[\frac{(\bar{\nu} - E_0 + \upsilon_M\hbar\omega_M)}{\Delta\bar{\nu}_{0,1/2}}\right]^2\right\}\right] \quad (3)$$

In eq 3, $I(\bar{\nu})$ is the relative emitted light intensity at energy $\bar{\nu}$ (in cm^{-1}), E_0 is the band maximum of the first member of the vibronic progression, υ_M is the vibrational quantum number for the medium frequency (ω_M) acceptor mode, S_M is the corresponding electron–vibrational coupling constant, and $\Delta\bar{\nu}_{0,1/2}$ is the bandwidth at half-maximum for the individual vibronic components which includes contributions from both solvent and low-frequency vibrations classically treated.[29] In the fitting procedure the quantum spacing of the medium-frequency acceptor mode was fixed at 1450 cm^{-1} as for $Ru(bpy)_2(CN)_2$. This averaged mode includes contributions from seven medium-frequency ν(bpy) modes and ν(CN). The parameters E_0, S_M, and $\Delta\bar{\nu}_{0,1/2}$ were varied to obtain the best fit. The results of the

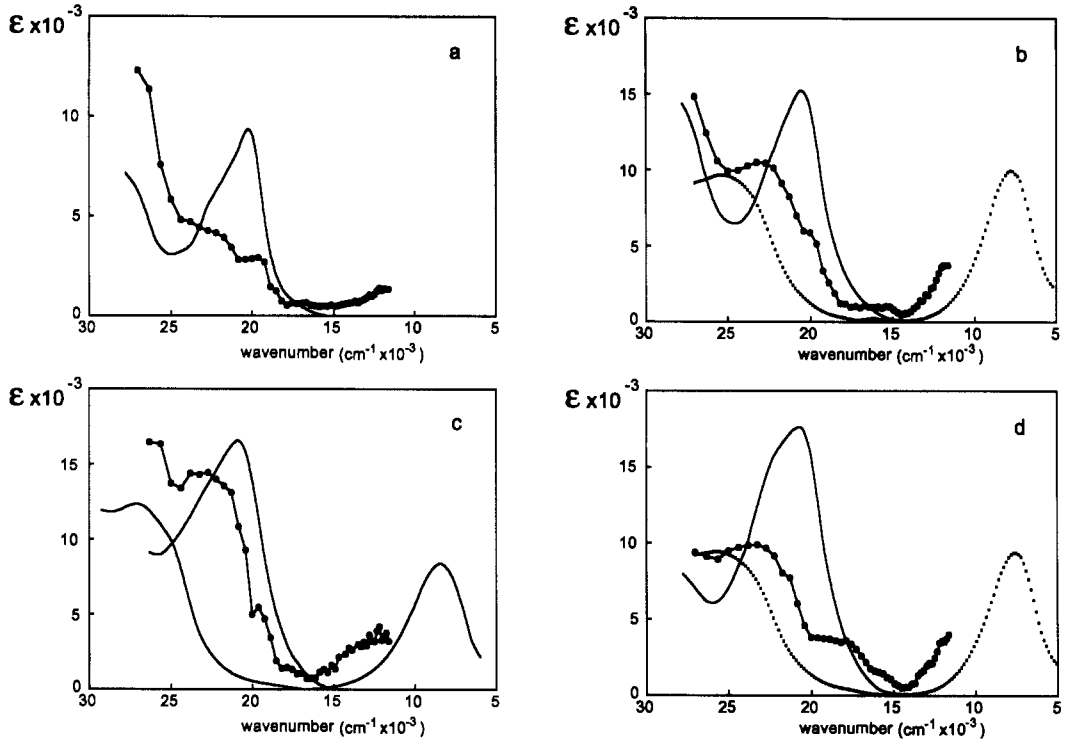

Figure 3. Absorption spectra in acetonitrile of reduced (—), one-electron oxidized (···) and electronically excited complexes (● – ●) for $Ru(bpy)_2(CN)_2$ (a), $[(NC)(bpy)_2Ru^{II}(CN)Ru^{II}(bpy)_2(CN)]^+$ (b), $[(NC)(bpy)_2Ru^{II}(CN)Ru^{II}(phen)_2(CN)]^+$ (c), and $[(NC)(phen)_2Ru^{II}(CN)Ru^{II}(bpy)_2(CN)]^+$ (d).

spectral fitting and photophysical data for the excited states are given in Table 1.

Laser Flash Photolysis. Transient absorption difference spectra were acquired on room-temperature acetonitrile solutions in the spectral range 370–860 nm. Transient absorption difference spectra for $Ru(bpy)_2(CN)_2$, $[(NC)(bpy)_2Ru^{II}(CN)Ru^{II}(bpy)_2(CN)]^+$, $[(NC)(bpy)_2Ru^{II}(CN)Ru^{II}(phen)_2(CN)]^+$, $[(NC)(phen)_2Ru^{II}(CN)Ru^{II}(bpy)_2(CN)]^+$, $[(NC)(bpy)_2Ru^{II}(CN)Ru^{II}(bpy)_2(NC)Ru^{II}(bpy)_2(CN)]^{2+}$, and $[(NC)(bpy)_2Ru^{II}(CN)Ru^{II}(dcb)_2(NC)Ru^{II}(bpy)_2(CN)]^{2-}$ are reported in Figures S1 and S2 (supplementary material). Common features in all these spectra are a bleach between 450 and 600 nm and positive absorption features in the regions 370–450 and 600–860 nm.

Ground- and excited-state spectra (ESA) of $Ru(bpy)_2(CN)_2$, $[(NC)(bpy)_2Ru^{II}(CN)Ru^{II}(bpy)_2(CN)]^+$, $[(NC)(phen)_2Ru^{II}(CN)Ru^{II}(bpy)_2(CN)]^+$, and $[(NC)(bpy)_2Ru^{II}(CN)Ru^{II}(phen)_2(CN)]^+$ are shown in Figure 3a–d. Ground and ESA spectra of $[(NC)(bpy)_2Ru^{II}(CN)Ru^{II}(bpy)_2(NC)Ru^{II}(bpy)_2(CN)]^{2+}$ and $[(NC)(bpy)_2Ru^{II}(CN)Ru^{II}(dcb)_2(NC)Ru^{II}(bpy)_2(CN)]^{2-}$ are shown in Figure 4a,c, respectively. The absorption spectra of the one-electron oxidized forms of the polynuclear complexes $[(NC)(bpy)_2Ru^{II}(CN)Ru^{III}(bpy)_2(CN)]^{2+}$, $[(NC)(phen)_2Ru^{II}(CN)Ru^{III}(bpy)_2(CN)]^{2+}$, $[(NC)(bpy)_2Ru^{II}(CN)Ru^{III}(phen)_2(CN)]^{2+}$, $[(NC)(bpy)_2Ru^{II}(CN)Ru^{III}(bpy)_2(NC)Ru^{II}(bpy)_2(CN)]^{3+}$, and $[(NC)(bpy)_2Ru^{II}(CN)Ru^{III}(dcb)_2(NC)Ru^{II}(bpy)_2(CN)]^-$ are also shown in Figures 3 and 4 for comparison.

Adducts with Zn^{2+}. In order to assign the electronic transitions underlying the ESA spectra of the polynuclear complexes (see Discussion), the spectroscopic and photophysical properties of adducts between $[(NC)(bpy)_2Ru^{II}(CN)Ru^{II}(bpy)_2(NC)Ru^{II}(bpy)_2(CN)]^{2+}$ and Zn^{2+} were investigated. In Figure 5 are shown spectra of acetonitrile solutions 5.9×10^{-5} M in $[(NC)(bpy)_2Ru^{II}(CN)Ru^{II}(bpy)_2(NC)Ru^{II}(bpy)_2(CN)]^{2+}$ with increasing amounts of $Zn(ClO_4)_2$. Isosbestic points at 388 and 441 nm (Figure 5a) were maintained from 0 to 3×10^{-5} M Zn^{2+}. A second set of isosbestic points at 371 and 424 nm (Figure 5b) were observed in the presence of higher concentrations (3×10^{-5} to 1.5×10^{-3} M) of Zn^{2+}. Further increases in Zn^{2+} had no effect. In spectrofluorimetric titrations, the emission maximum for $[(NC)(bpy)_2Ru^{II}(CN)Ru^{II}(bpy)_2(NC)Ru^{II}(bpy)_2(CN)]^{2+}$ shifted to higher energy with a parallel enhancement in emission intensity and lifetime. The limiting values for the emission maxima and lifetimes in the presence of a 25-fold excess of Zn^{2+} are reported in Table 1.

Transient absorbance measurements were made on solutions having the same concentration of Zn^{2+}. The transient absorption difference spectrum of $[(NC)(bpy)_2Ru^{II}(CN)Ru^{II}(bpy)_2(NC)Ru^{II}(bpy)_2(CN)]^{2+}$ in the presence of a 25-fold excess of Zn^{2+} is shown in Figure S2b. In Figure 4b the calculated ESA spectrum and the ground-state absorption spectrum before and after addition of excess of Br_2 are shown.

In cyclic voltammetric measurements, addition of a 25-fold excess of $Zn(ClO_4)_2$ to acetonitrile solutions containing $[(NC)(bpy)_2Ru^{II}(CN)Ru^{II}(bpy)_2(NC)Ru^{II}(bpy)_2(CN)]^{2+}$ shifted the three $Ru^{III/II}$ oxidation waves from $E_{1/2}$ = 0.66, 1.19, and 1.46 V to $E_{1/2}$ = 0.75, 1.47, and 1.64 V.

Discussion

Excited-State Raman Spectra. We recently reported an investigation of the mixed-valence complex $[(NC)(bpy)_2Ru^{II}(CN)Ru^{III}(bpy)_2(CN)]^{2+}$ in which infrared and resonance Raman data supported valence localization.[22] The time-resolved infrared spectrum of $[(NC)(bpy)_2Ru^{II}(CN)Ru^{II}(bpy)_2(CN)]^+$ following MLCT excitation suggested localization in the excited state as well. In the transient IR difference spectrum, three ν(CN) bands appear for the excited state at energies comparable to those exhibited by $[(NC)(bpy)_2Ru^{II}(CN)Ru^{III}(bpy)_2(CN)]^{2+}$. The similarity in band energies suggests a similar distribution of electron density at the metals in the mixed-valence and the excited-state complex.

To clarify this result and gain further insight into the nature of the excited state following MLCT excitation of $[(NC)(bpy)_2Ru^{II}(CN)Ru^{II}(bpy)_2(CN)]^+$, we have utilized time-resolved resonance Raman spectroscopy and the complexes $[(NC)(phen)_2Ru^{II}(CN)Ru^{II}(bpy)_2(CN)]^+$ and $[(NC)(bpy)_2Ru^{II}(CN)$-

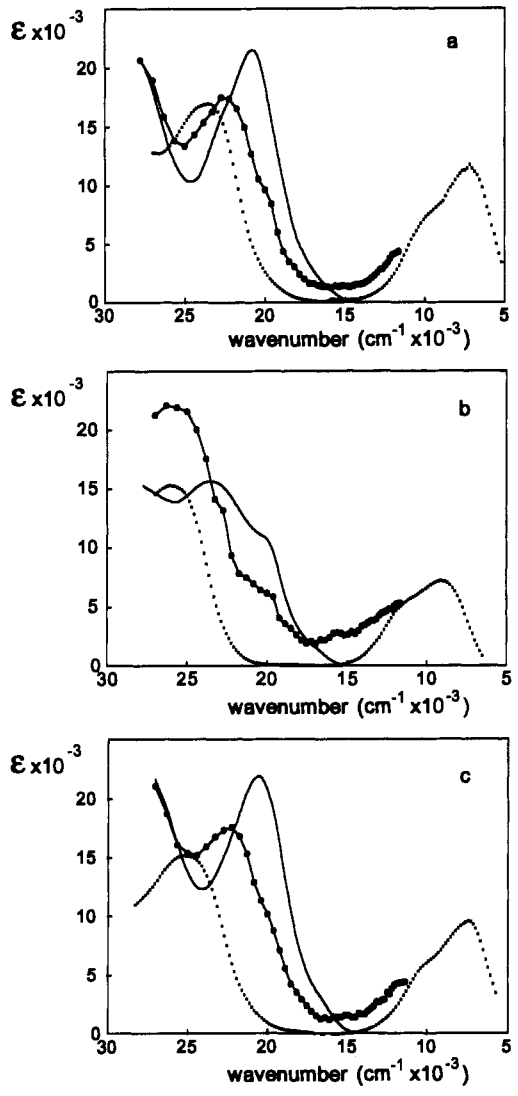

Figure 4. Absorption spectra in acetonitrile of reduced (—), one-electron oxidized (···) and electronically excited complexes (● – ●) for $[(NC)(bpy)_2Ru^{II}(CN)Ru^{II}(bpy)_2(NC)Ru^{II}(bpy)_2(CN)]^{2+}$ (a), $[Zn(NC)(bpy)_2Ru^{II}(CN)Ru^{II}(bpy)_2(NC)Ru^{II}(bpy)_2(CN)Zn]^{6+}$ (b), and $[(NC)(bpy)_2Ru^{II}(CN)Ru^{II}(dcb)_2(NC)Ru^{II}(bpy)_2(CN)]^{2-}$ (c). The spectrum of the oxidized complex $[(NC)(bpy)_2Ru^{II}(CN)Ru^{III}(dcb)_2(NC)Ru^{II}(bpy)_2(CN)]^-$ was obtained in D_2O (see Experimental Section).

$Ru^{II}(phen)_2(CN)]^+$. The exchange of phen for bpy is nearly isomorphous electronically as shown for example by the properties of $Ru(phen)_2(CN)_2$ compared to $Ru(bpy)_2(CN)_2$ (Table 1) and by the similarity of the HOMO and LUMO orbitals of H_2bpy^{2+} and H_2phen^{2+},[38] and yet the two ligands can be distinguished unambiguously by the resonance Raman technique.

The data in Figure 1 and Table 2 clearly demonstrate that substantial differences exist between the transient Raman spectra of $[(NC)(phen)_2Ru^{II}(CN)Ru^{II}(bpy)_2(CN)]^{+*}$ and $[(NC)(bpy)_2Ru^{II}(CN)Ru^{II}(phen)_2(CN)]^{+*}$. The spectrum of the former is essentially that for $bpy^{\bullet-}$ in $[Ru(bpy)_3]^{2+*}$,[33-35] with the only features associated with the phen ligand arising from enhancement of ground-state signals. This result is consistent with the assignment of the lowest excited state on the nanosecond time scale as $[(NC)(phen)_2Ru^{II}(CN)Ru^{III}(bpy)(bpy^{\bullet-})(CN)]^+$. This state is reached both directly by excitation and indirectly by energy transfer following $Ru^{II} \rightarrow$ phen excitation (Scheme 1).

The transient Raman spectrum of $[(NC)(bpy)_2Ru^{II}(CN)Ru^{II}(phen)_2(CN)]^{+*}$ is dominated by the ground-state ν(bpy) bands which gain enhancement from the ground-state $\pi \rightarrow \pi^*$ absorption near 320 nm. However, bands which are assignable to $phen^{\bullet-}$ by

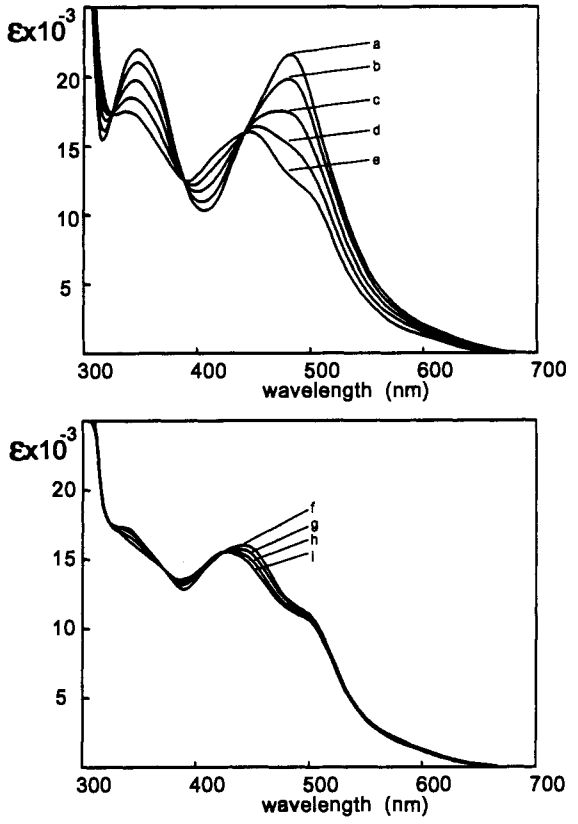

Figure 5. Absorption spectra in acetonitrile 5.9×10^{-5} M in $[(NC)(bpy)_2Ru^{II}(CN)Ru^{II}(bpy)_2(NC)Ru^{II}(bpy)_2(CN)]^{2+}$ (a) and increasing amounts of $Zn(ClO_4)$: 5×10^{-6} M (b); 1×10^{-5} M (c); 1.5×10^{-5} M (d); 3×10^{-5} M (e); (f) 5×10^{-5} M (g); 7.5×10^{-5} M (h); 1.4×10^{-4} M (i); 1.5×10^{-3} M (i).

comparison to $[Ru(phen)_3]^{2+*}$ are clearly discernible at 1315, 1432, 1455, and 1515 cm^{-1}. The simultaneous intense ground-state features for the bpy ligand and the excited-state features for phen are consistent with the oxidation state distribution $[(NC)(bpy)_2Ru^{II}(CN)Ru^{III}(phen)(phen^{\bullet-})(CN)]^+$ as the primary component on the time scale of the experiment (about 7 ns).

The oxidation-state distribution revealed by the transient spectrum of $[(NC)(bpy)_2Ru^{II}(CN)Ru^{II}(dcb)_2(NC)Ru^{II}(bpy)_2(CN)]^{2-}$ is consistent with the role of the bridge asymmetry in providing part of the driving force for energy transfer.[23] The spectrum (Figure 2) lacks the typical intense Raman bands for $bpy^{\bullet-}$ at 745, 1212, 1285, 1424, and 1549 cm^{-1}. Bands due to ground-state bpy vibrations are evident in the spectrum most notably at 1561 and 1605 cm^{-1}. Clear evidence that energy transfer has occurred to the inner Ru is shown by the presence of bands at 1113, 1289, and 1446 cm^{-1} for $dcb^{\bullet-}$ which appear in the transient spectra of $[Ru^{II}(dcb)_2(CN)_2]^{4-}$ (Table 3) and $[Ru^{II}(dcbH_2)_3]^{2+}$.[39]

Electronic Absorption Spectra of the Excited States. The coincidence of the decay rate constants for the transient absorption and emission decays are consistent with lowest ^{3}MLCT excited states in all cases. The transient absorbance difference spectrum of $Ru(bpy)_2(CN)_2$, following excitation at 354.7 nm in aqueous solution, has previously been investigated.[40] The main difference between the spectrum in Figure S1a, which was measured in acetonitrile, and the previously reported spectrum is the appearance of a transient absorption feature at 700 nm in water. This feature was reported to decay with a rate proportional to the concentration of complex and was attributed to hydrated electrons.[40] The ESA spectrum of $Ru(bpy)_2(CN)_2$ in acetonitrile

(38) Kober, E. M.; Meyer, T. J. *Inorg. Chem.* **1985**, *24*, 106.

(39) Yabe, T.; Orman, L. K.; Anderson, D. R.; Yu, S.-C.; Xu, X.; Hopkins, J. B. *J. Phys. Chem.* **1990**, *94*, 7128.

(40) Atherton, S. J. *J. Phys. Chem.* **1984**, *88*, 2840.

(Figure 3a) includes bands between 18×10^3 and 27×10^3 cm^{-1} which are similar in energy and intensity to those observed for the ^{3}MLCT excited state of $[Ru(bpy)_3]^{2+}$ [41-43] and $Ru(bpy)(CN)_4^{2-}$ [44] and resemble those of the $bpy^{\bullet-}$ radical anion.[45] The low-energy band, which is evident up to 11.5×10^3 cm^{-1}, has also been observed for the one-electron reduced complexes $Ru^{II}(bpy)_3^+$ [46] and $Ir^{II}(bpy)_3^+$.[47] On the basis of these comparisons, this absorbance feature in the ESA spectrum of $Ru(bpy)_2(CN)_2$ can be attributed to a $bpy^{\bullet-}$-localized $\pi \rightarrow \pi^*$ transition.

In the ESA spectra of the binuclear and trinuclear complexes, Figures 3b–d and 4a,c, additional intense bands appear in the visible region compared to those for $Ru(bpy)_2(CN)_2$*. The inherent redox asymmetry imposed by the cyano bridge makes the contribution to the ESA spectra from ^{3}MLCT excited states localized on C-bonded (to bridging CN^-) chromophores negligible, consistent with the excited-state Raman results. For $[(NC)(bpy)_2Ru^{II}(CN)Ru^{II}(bpy)_2(NC)Ru^{II}(bpy)_2(CN)]^{2+}$ the lower energy excited state, $[(NC)(bpy)_2Ru^{II}(CN)Ru^{III}(bpy^-)(bpy)(NC)Ru^{II}(bpy)_2(CN)]^{2+}$, should exhibit absorption bands arising from ligand-localized π–$\pi^*(bpy^{\bullet-})$ transitions and charge-transfer transitions similar to those that appear in the mixed-valence complex $[(NC)Ru^{II}(bpy)_2(CN)Ru^{III}(bpy)_2(NC)Ru^{II}(bpy)_2(CN)]^{3+}$.[20,22] These include $d\pi \rightarrow \pi^*(bpy)$ transitions localized on the external $-(NC)Ru^{II}(bpy)_2(CN)$ units and an intervalence Ru(II) → Ru(III) transition (IT). Ligand to metal charge-transfer bands, $\pi \rightarrow d\pi$ (bpy → Ru(III))[48,49] or (CN → Ru(III)),[50] are also expected to contribute to the absorption spectrum of the mixed-valence complexes. These bands tend to be of relatively low intensity and are expected to be masked by the more intense MLCT bands.

The comparison of the ESA spectrum of $[(NC)(bpy)_2Ru^{II}(CN)Ru^{II}(bpy)_2(NC)Ru^{II}(bpy)_2(CN)]^{2+}$ with ground-state spectra of reduced and one-electron oxidized forms (Figure 4a) suggests that the band at 22.5×10^3 cm^{-1}, in the excited state, originates from the additive contribution of MLCT transitions localized on the two $-(NC)Ru^{II}(bpy)_2(CN)$ units and π–$\pi^*(bpy^{\bullet-})$ transitions. The energy of this band is intermediate between those of the MLCT bands for $[(NC)(bpy)_2Ru^{II}(CN)Ru^{III}(bpy)_2(NC)Ru^{II}(bpy)_2(CN)]^{3+}$ at 23.6×10^3 cm^{-1} and $[(NC)(bpy)_2Ru^{II}(CN)Ru^{II}(bpy)_2(NC)Ru^{II}(bpy)_2(CN)]^{2+}$ at 20.9×10^3 cm^{-1}. This difference is due to electronic perturbation by the excited $Ru^{III}(bpy^{\bullet-})$ unit on the adjacent $-(NC)Ru^{II}(bpy)_2(CN)$ chromophore. The effect is less than that produced by the presence of a Ru^{III} center,[22] due to partial delocalization of the electron on the bpy ligand into the $d\pi$ metal orbitals. Time-resolved resonance Raman spectroscopy has shown for a series of Os and Ru complexes that the extent of charge transfer in the MLCT excited state is less than a complete electron unit.[51] The shift observed between the MLCT bands for the ground and excited states is qualitatively consistent with this result.

The red absorption, from 600 to 860 nm, observed in the excited state of $[(NC)(bpy)_2Ru^{II}(CN)Ru^{II}(bpy)_2(NC)Ru^{II}(bpy)_2(CN)]^{2+}$ is about three times more intense than the band exhibited by $Ru(bpy)_2(CN)_2$. The additional intensity may arise from another transition which adds to the intensity contributed by π–$\pi^*(bpy^-)$ transition(s). Some insight as to the origin of the intensity can be obtained from the spectral variations observed following the addition of Zn^{2+} to acetonitrile solutions of $[(NC)Ru^{II}(bpy)_2(CN)Ru^{II}(bpy)_2(NC)Ru^{II}(bpy)_2(CN)]^{2+}$ (Figure 5). In $[(NC)(bpy)_2Ru^{II}(CN)Ru^{II}(bpy)_2(NC)Ru^{II}(bpy)_2(CN)]^{2+}$ the emitting central unit is protected from interaction with Zn^{2+} ions, while the external $-(NC)Ru(bpy)_2(CN)$ units have unbound cyano ligands available for binding the metal cations.[52-54] The limiting absorption spectrum obtained in the presence of a 25-fold excess of Zn^{2+} is consistent with formation of an adduct in which the cyano groups of both peripheral units are bound to Zn^{2+} ions, $[Zn^{II}(NC)Ru^{II}(bpy)_2(CN)Ru^{II}(bpy)_2(NC)Ru^{II}(bpy)_2(CN)Zn^{II}]^{6+}$. The interaction of cyano complexes of ruthenium(II) with metal ions or molecules acting as Lewis acids causes a positive shfit of $E^{ox}_{1/2}$ for the $Ru^{III/II}$ couples which is accompanied by a nearly proportional increase in the energy of the MLCT manifold.[16,52-54] For $[(NC)(bpy)_2Ru^{II}(CN)Ru^{II}(bpy)_2(NC)Ru^{II}(bpy)_2(CN)]^{2+}$, the shift in $E^{ox}_{1/2}(2)$ and $E^{ox}_{1/2}(3)$ (Table 1) in the presence of Zn^{2+} are comparable in magnitude to the energy difference between MLCT band maxima in the presence and absence of Zn^{2+}. On this basis, the intense band at 430 nm in the absorption spectrum of $[Zn^{II}(NC)Ru^{II}(bpy)_2(CN)Ru^{II}(bpy)_2(NC)Ru^{II}(bpy)_2(CN)Zn^{II}]^{6+}$ is assigned to the MLCT transitions localized on the external units with the pronounced shoulder at 500 nm originating from the central unit $-(CN)Ru^{II}(bpy)_2(NC)-$.

Addition of Br_2 to acetonitrile solutions of $[Zn^{II}(NC)(bpy)_2Ru^{II}(CN)Ru^{II}(bpy)_2(NC)Ru^{II}(bpy)_2(CN)Zn^{II}]^{6+}$ leads to quantitative oxidation of the central ruthenium to Ru(III) as demonstrated by the presence of isosbestic points during the titration. The absorptivity and half-width of the IT band at 8800 cm^{-1} (Figure 4b) are similar to the IT band observed for $[(NC)(bpy)_2Ru^{II}(CN)Ru^{III}(bpy)_2(NC)Ru^{II}(bpy)_2(CN)]^{3+}$ at 7250 cm^{-1} (Figure 4a). In the limit of weak electronic coupling between the metal centers, the optical energy (E_{op}) of the IT band connecting the different oxidation state isomers (eqs 4 and 5) is related to the free energy difference between the different

$$[(NC)(bpy)_2Ru^{II}(CN)Ru^{III}(bpy)_2(NC)Ru^{II}(bpy)_2(CN)]^{3+} \xrightarrow{h\nu} [(NC)(bpy)_2Ru^{III}(CN)Ru^{II}(bpy)_2(NC)Ru^{II}(bpy)_2(CN)]^{3+} \quad (4)$$

$$[Zn^{II}(NC)(bpy)_2Ru^{II}(CN)Ru^{III}(bpy)_2(NC)Ru^{II}(bpy)_2(CN)Zn^{II}]^{7+} \xrightarrow{h\nu} [Zn^{II}(NC)(bpy)_2Ru^{III}(CN)Ru^{II}(bpy)_2(NC)Ru^{II}(bpy)_2(CN)Zn^{II}]^{7+} \quad (5)$$

oxidation state isomers ($\Delta G°$) and the total (inner and outer sphere) reorganizational energy, χ, by

$$E_{op} = \Delta G° + \chi \quad (6)$$

$$E_{op}' = \Delta G°' + \chi' \quad (7)$$

On the basis of a thermochemical analysis, the difference between E_{op} for Ru(II)–Ru(III) and Ru(II)–Os(III) complexes connected by the same asymmetrical bridge corresponds to the difference between their $\Delta E_{1/2}$ values, $\Delta(\Delta E_{1/2})$.[55] The quantity $\Delta E_{1/2}$ is the difference between the $E_{1/2}$ values of the consecutive one-electron oxidations at the two metal sites in each dimer. Using

(41) Watts, R. J. *J. Chem. Educ.* **1983**, *10*, 835.
(42) Creutz, C.; Chou, M.; Netzel, T. L.; Okumura, M.; Sutin, N. *J. Am. Chem. Soc.* **1980**, *102*, 1309.
(43) Braterman, P. S.; Harriman, A.; Heath, G. A.; Yellowlees, L. J. *J. Chem. Soc., Dalton Trans.* **1983**, 1801.
(44) Bignozzi, C. A.; Chiorboli, C.; Indelli, M. T.; Rampi, M. A.; Varani, G.; Scandola, F. *J. Am. Chem. Soc.* **1986**, *108*, 7872.
(45) (a) Mahon, C.; Reynolds, W. L. *Inorg. Chem.* **1967**, *6*, 1927. (b) Mulazzani, Q. G.; Emmi, S.; Fuochi, P. G.; Venturi, M.; Hoffman, M. Z.; Simic, M. G. *J. Phys. Chem.* **1979**, *12*, 1582.
(46) Heath, G. A.; Yellowlees, L. J. *J. Chem. Soc., Chem. Commun.* **1981**, 287.
(47) Coombe, V. T.; Heath, G. A.; MacKenzie, A. J.; Yellowlees, L. J. *Inorg. Chem.* **1984**, *23*, 3423.
(48) Johnson, E. C.; Callahan, R. W.; Eckberg, R. P.; Hatfield, W. E.; Meyer, T. J. *Inorg. Chem.* **1979**, *18*, 618.
(49) (a) Bryant, G. M.; Fergusson, J. E. *Aust. J. Chem.* **1971**, *24*, 275. (b) McCaffery, A. J.; Mason, S. F.; Norman, B. J. *J. Chem. Soc. A* **1969**, 1428.
(50) Vogler, A.; Kunkely, H. *Inorg. Chim. Acta* **1981**, *53*, L215.
(51) Caspar, J. V.; Westmoreland, T. D.; Allen, G. H.; Bradley, P. G.; Meyer, T. J.; Woodruff, W. H. *J. Am. Chem. Soc.* **1984**, *106*, 3492.
(52) Demas, J. N.; Addinghton, J. W.; Peterson, S. H.; Harris, E. W. *J. Phys. Chem.* **1977**, *81*, 1039.
(53) Whitten, D. G.; Kinnaird, M. G. *Chem. Phys. Lett.* **1982**, *88*, 275.
(54) Scandola, F.; Bignozzi, C. A. In *Supramolecular Photochemistry*; Balzani, V., Ed.; Reidel: Dordrecht, The Netherlands, 1987; p 121.
(55) Goldsby, K. A.; Meyer, T. J. *Inorg. Chem.* **1984**, *23*, 3002.

analogous arguments for the mixed-valence ions $[(NC)(bpy)_2Ru^{II}(CN)Ru^{III}(bpy)_2(NC)Ru^{II}(bpy)_2(CN)]^{3+}$ and $[Zn^{II}(NC)(bpy)_2Ru^{II}(CN)Ru^{III}(bpy)_2(NC)Ru^{II}(bpy)_2(CN)Zn^{II}]^{7+}$ and the $E^{ox}_{1/2}(1)$ and $E^{ox}_{1/2}(2)$ values of Table 1, the calculated difference between $\Delta E_{1/2}$ for $[Zn^{II}(NC)Ru^{II}(bpy)_2(CN)Ru^{II}(bpy)_2(NC)Ru^{II}(bpy)_2(CN)Zn^{II}]^{6+}$ and $[(NC)Ru^{II}(bpy)_2(CN)Ru^{II}(bpy)_2(NC)Ru^{II}(bpy)_2(CN)]^{2+}$, $\Delta(\Delta E_{1/2})$, is 0.21 V. This value is comparable within experimental error to ΔE_{op} = 0.19 eV, suggesting that for these ions E_{op} varies with $\Delta G°$ as predicted.

Extension of these arguments to the low-energy absorption features in the ESA spectra of the polynuclear complexes requires the assumption that the electronic coupling and reorganizational energy do not differ substantially from the ground state. By comparison of spectra for $[Zn^{II}(NC)Ru^{II}(bpy)_2(CN)Ru^{II}(bpy)_2(NC)Ru^{II}(bpy)_2(CN)Zn^{II}]^{6+}$ (Figure 4b) and $[(NC)Ru^{II}(bpy)_2(CN)Ru^{II}(bpy)_2(NC)Ru^{II}(bpy)_2(CN)]^{2+}$ (Figure 4a), it is evident that the absorption bands in $[Zn^{II}(NC)Ru^{II}(bpy)_2(CN)Ru^{II}(bpy)_2(NC)Ru^{II}(bpy)_2(CN)Zn^{II}]^{6+}$ are at higher energy. This shift is expected qualitatively by $\Delta G°$ of the optical energies of the MLCT and IT transitions. Given the difference in $E_{1/2}$ for the first $Ru^{III/II}$ waves and the calculated excited-state reduction potentials $^*E^{red}_{1/2}$ (Table 1), enegy shifts in the range 1700–2500 cm^{-1} are expected for excited-state IT absorption compared to ground state. The fact that in all cases the band profiles of the low-energy absorption feature observed in the ESA spectra parallel the ground-state IT bands with positive shifts on the order of ca. 1000–2000 cm^{-1} (Figures 3 and 4) supports the assignment of these absorption features to the onset of excited-state IT bands. These conclusions are in agreement with the spectral features observed in the transient absorption spectra of complexes of the type $[(bpy)(CO)_3Re^{I}(CN)Ru^{II}(dcb)_2(NC)Re^{I}(CO)_3(bpy)]^{2+}$ [4c] and $[(NC)(bpy)_2Ru^{II}(CN)Ru^{II}(dcb)_2(NC)Ru^{II}(bpy)_2(CN)]^{2-}$,[56] for which the band shape of the excited-state IT was defined in the 700–1200-nm spectral range.

Conclusions

Despite the relatively large electronic coupling provided by the bridging cyanide ligand, the polychromophoric complexes of the type $[(NC)(NN)_2Ru^{II}(CN)Ru^{II}(NN)_2(CN)]^{+}$ (NN = bpy, phen) and $[(NC)(NN)_2Ru^{II}(CN)Ru^{II}(NN)_2(NC)Ru(NN)_2(CN)]^{2+}$ and $[(NC)(NN)_2Ru^{II}(CN)Ru^{II}(NN')_2(NC)Ru^{II}(NN)_2(CN)]^{2-}$ (NN = bpy, NN′ = dcb) have essentially valence-localized ground states.[20,22,23] In this work, two basic questions concerning the *electronically excited states* of these complexes have been addressed: (i) Are the excited states localized on a single molecular component or delocalized? (ii) If they are localized, which molecular component has the lowest-energy excited state? These two questions have been addressed with the aid of transient resonance Raman and transient UV/vis absorption spectroscopies.

In mononuclear Ru(II) polypyridine complexes, the excited states are of the MLCT type, implying the presence of the oxidized metal center and of a reduced polypyridine ligand. Thus, the question of localization *vs* delocalization in the excited states of the polynuclear complexes reduces to the following: (ia) Is the promoted electron resident on the polypyridine ligands of a single metal or delocalized over different molecular components? (ib) Are the metal centers individually or collectively oxidized? The first point has been answered and localization established by the use of transient resonance Raman spectroscopy. The observation in every case of vibrations of a single type of (reduced) ligand and the cross check obtained by exchanging ligands and metal centers provide unambiguous evidence for localization of the excited electron. The second point has been addressed using transient absorption spectroscopy. The observation of intervalence transfer transitions unequivocally demonstrates the presence of distinct Ru(II) and Ru(III) centers in the excited state of the polynuclear complexes.

The effect of the binding mode of cyanide on the relative energy ordering of the MLCT states in cyano-bridged polynuclear complexes of this type has been previously inferred from indirect evidence (correlation between emission energies of different complexes, electrochemical data).[20,22] In this work the energy ordering has been established experimentally by transient resonance Raman measurements. In all cases, these experiments label the lowest excited state (reached by fast intercomponent energy transfer) as the Ru(II) center with the largest number of N-bonded cyanide ligands.

Acknowledgment. The Italian portion of this work was supported by the Ministero della Università e della Ricerca Scientifica e Tecnologica and by the Consiglio Nazionale delle Ricerche (Progetto Finalizzato Chimica Fine). The work at UNC was supported by the Department of Energy Grant DOE-FG05-86ER13633 to T.J.M. Part of this work was performed at Los Alamos National Laboratory under the auspices of the U.S. Department of Energy.

Supplementary Material Available: Transient absorption spectra of $Ru(bpy)_2(CN)_2$, $[(NC)(bpy)_2Ru^{II}(CN)Ru^{II}(bpy)_2(CN)]^{+}$, $[(NC)(bpy)_2Ru^{II}(CN)Ru^{II}(phen)_2(CN)]^{+}$, and $[(NC)(phen)_2Ru^{II}(CN)Ru^{II}(bpy)_2(CN)]^{+}$ in acetonitrile (Figure S1) and transient absorption spectra of $[(NC)(bpy)_2Ru^{II}(CN)Ru^{II}(bpy)_2(NC)Ru^{II}(bpy)_2(CN)]^{2+}$, $[Zn(NC)(bpy)_2Ru^{II}(CN)Ru^{II}(bpy)_2(NC)Ru^{II}(bpy)_2(CN)Zn]^{6+}$, and $[(NC)(bpy)_2Ru^{II}(CN)Ru^{II}(dcb)_2(NC)Ru^{II}(bpy)_2(CN)]^{2-}$ in acetonitrile (Figure S2) (2 pages). Ordering information is given on any current masthead page.

(56) Matsui, K.; Nazeeruddin, Md. K.; Baker, R. H.; Gratzel, M.; Kalyanasundaram, K. *J. Phys. Chem.* **1992**, *96*, 10587.